Title

Modulating the sEH/EETs Axis Restrains Specialized Proresolving Mediator Impairment and Regulates T Cell Imbalance in Experimental Periodontitis.

Journal

The Journal of Immunology, 212(3)

ISSN

0022-1767

Authors

Abdalla, Henrique B

Puhl, Luciano

Rivas, Carla Alvarez

et al.

Publication Date

2024-02-01

DOI

10.4049/jimmunol.2300650

Peer reviewed

Published in final edited form as:

J Immunol. 2024 February 01; 212(3): 433–445. doi:10.4049/jimmunol.2300650.

Modulating the sEH/EETs axis restrains Specialized Pro-Resolving Mediator impairment and regulates T-cell imbalance in experimental periodontitis

Henrique B. Abdalla[*,†], **Luciano Puhl**[†], **Carla Alvarez Rivas**[*,‡], **Yu-Chiao Wu**[*,‡], **Paola Rojas**[*], **Carlos Antonio Trindade-da-Silva**[†], **Bruce D. Hammock**[§], **Krishna R. Maddipati**[¶], **Mariana Q. S. Soares**[‖], **Juliana T. Clemente-Napimoga**[†], **Alpdogan Kantarci**[*], **Marcelo H. Napimoga**[†,1], **Thomas E. Van Dyke**[*,#,1]

[*]Department of Applied Oral Sciences, The Forsyth Institute, Cambridge, MA, USA.

[†]Faculdade São Leopoldo Mandic, Campinas, SP, Brazil.

[‡]Harvard School of Dental Medicine, Boston, MA, USA.

[§]Department of Entomology and UCD Comprehensive Cancer Center, University of California, Davis, CA, USA.

[¶]Department of Pathology, Wayne State University, Detroit, MI, USA.

[‖]Division of Oral Radiology, Faculdade São Leopoldo Mandic, Campinas, Brazil.

[#]Department of Oral Medicine, Infection, and Immunity, Faculty of Medicine, Harvard University, Boston, MA, USA.

Abstract

Epoxyeicosatrienoic acids (EETs) and other epoxy fatty acids (EpFAs) are short-acting lipids involved in resolution of inflammation. Their short half-life, due to its metabolism by soluble epoxide hydrolase (sEH), limits their effects. Specialized pro-resolving mediators (SPMs) are endogenous regulatory lipids insufficiently synthesized in uncontrolled and chronic inflammation. Using an experimental periodontitis model, we pharmacologically inhibited sEH, examining its impact on T-cell activation and systemic SPM production. In humans, we analyzed sEH in the gingival tissue of periodontitis patients. Mice were treated with sEHi and/or EETs before ligature placement and treated for 14 days. Bone parameters were assessed by μCT and methylene blue staining. Blood plasma metabololipidomics were carried out to quantify SPM levels. We also determined T-cell activation by RT-qPCR and Flow Cytometry in cervical lymph nodes. Human gingival samples were collected to analyze sEH using ELISA and Electrophoresis. Data reveal that pharmacological sEHi abrogated bone resorption and preserved bone architecture. Metabolipidomics revealed that sEHi enhances Lipoxin (LX) A4, LXB4, resolvin (Rv) E2, and

[1]**To whom correspondence may be addressed:** Dr. Thomas E. Van Dyke, Forsyth Institute, Cambridge, MA 02142. tvandyke@forsyth.org; marcelo.napimoga@slmandic.edu.br.

Disclosures

Dr. Van Dyke is an inventor of several granted and pending licensed and unlicensed patents awarded to the Forsyth Institute that are subject to consulting fees and royalty payments. B.D. Hammock is inventor on a University of California patent for synthesis and application of sEH inhibitors for disease treatment. All other authors declare that they have no competing interests.

RvD6. An increased percentage of regulatory T-cells over Th17 was noted in sEHi-treated mice. Lastly, inflamed human gingival tissues presented higher levels and expression of sEH than healthy gingivae, being positively correlated with periodontitis severity. Our findings indicate that sEHi preserves bone architecture and stimulate SPM production, associated with regulatory actions on T-cells favoring resolution of inflammation. Since sEH is enhanced in human gingivae from patients with periodontitis and connected with disease severity, inhibition may prove to be an attractive target for managing osteolytic inflammatory diseases.

Keywords

Soluble Epoxide Hydrolase; Specialized Pro-Resolving Mediators; Periodontitis; Inflammation; Lymphocytes

INTRODUCTION

Periodontitis is one of the most prevalent inflammatory disorders that affects the oral cavity (1), induced by interactions between the host immune response and the dysbiotic plaque biofilm. Epidemiologically, severe periodontitis has substantially increased over the past three decades, reaching 1.1 billion cases worldwide (2). Clinically, it is characterized by the progressive destruction of hard and soft tissue, bleeding of the gums, and tooth loss (3). Furthermore, as a consequence of the uncontrolled inflammatory process, a shift occurs from the innate to the adaptative immune system (4). After the initial influx of circulating leukocytes (neutrophils and monocytes) and the expansion of resident macrophages (acquiring inflammatory phenotype), CD4+ T-cells become important pathogenic drivers of the osteolytic inflammatory milieu, especially by IL-17-producing CD4+ helper T cells, named Th17 cells (5). Th17 cells produce IL-17A that triggers the production of reactive oxygen species (ROS) and neutrophil extracellular traps (NETs), and mediates bone resorption (6; 7). On the other hand, regulatory T-cells (Treg) possess immunomodulatory functions, preventing the exaggerated inflammatory reaction. Notably, these regulatory actions are due to the impact on effector cells, such as neutrophils, macrophages, and T and B cells (8). The imbalance between Th17/Treg is partially responsible for the bone resorption induced by periodontitis, which is critical in its pathogenesis (9).

Resolution of inflammation is characterized by a highly orchestrated process that switches lipid mediator production from classic inflammatory mediators (e.g., prostaglandins and leukotrienes), to gradual enhancement of pro-resolution mediators, such as lipoxins, resolvins, and protectins (10; 11; 12). These resolution lipid mediators are called Specialized Pro-Resolving Mediators (SPMs). SPMs are bioactive lipid mediators synthesized from polyunsaturated fatty acids (e.g., ω-3 and −6 fatty acids) during the resolution phase of inflammation and act as stop signals for the acute inflammatory response and assist to coordinate the resolution process (13). Furthermore, eicosanoids are lipid mediators from the metabolism of arachidonic acid (ARA) by the cyclooxygenases (COX), lipoxygenases (LOX), or cytochrome P450 (CYP450) (14; 15). The resulting bioactive lipids (e.g., prostanoids, leukotrienes, and epoxyeicosatrienoic acids [EETs]) have a dual role in inflammation (16).

Specifically, the EETs, like other long-chain polyunsaturated fatty acids (EpFA) generated by the cytochrome P450 pathway, are bioactive lipids with immunomodulatory functions during inflammation (17). However, many of these lipid mediators are short-lived due to their quick conversion into inactive diols in the presence of soluble epoxide hydrolase (sEH) (18). Additionally, these diols contribute to inflammatory cytokine production and prevent the beginning of the resolution phase (19). The sEH enzymes are detected in many organs (20; 21; 22; 23), and high sEH expression was observed in chronic stages of inflammation. Importantly, the equilibrium between pro-inflammatory and pro-resolving mediators is necessary for maintaining coordinated immune responses and the dysregulation of SPM production drives chronic inflammation.

Therefore, the current study examined the influence of the modulation of the sEH/EET axis on the alveolar bone architecture in experimental periodontitis. Using metabolipidomics, we looked at the SPM profile in blood serum and investigated the T-cell profile in cervical lymph nodes that drain periodontal areas.

MATERIAL AND METHODS

Drugs

TPPU was used as the sEH inhibitor. 1-(1-propanoylpiperidin-4-yl)-3-[4-(trifluoromethoxy)phenyl]urea (TPPU) was synthesized at the Department of Entomology and Nematology, University of California-Davis (USA) as previously published (24). sEH was dissolved in polyethylene glycol 400 (PEG400; Sigma) in the respective working dosages. Sonification was used for the total dissolution of sEHi. Likewise, the mixture of EET regioisomers (5,6-EET, 8,9-EET, 11,12-EET, and 14,15-EET) was synthesized at the Department of Entomology and Nematology, University of California-Davis (USA), using procedures published elsewhere (25). The EET stock solution (10 mM diluted in DMSO) was maintained at −80°C. EETs were thawed and dissolved in PEG400 at a 1 μg/kg dose for each experiment.

Animals Approval and Care

Male C57BL/6 mice (25–30 grams) were used in this study. Animals were purchased from Jackson Laboratory and randomly allocated in plastic cages (n = 5/per cage) in a temperature-controlled room (23 ± 1°C) in a pathogen-free environment, 12:12 light cycle, with access to water and food *ad libitum*. All animal experimentation was authorized by the Institutional Animal Care and Use Committee of the Forsyth Institute (#17-020) and is reported in compliance with the ARRIVE guidelines (26). All efforts were made to minimize animal suffering and to reduce the number of animals used. Each experimental group had 5 animals per experiment.

Experimental Periodontitis Protocol and Treatment Regimens

For the induction of experimental periodontitis, animals were initially anesthetized with ketamine (10ml/kg) and xylazine (0.86 mg/ml) intraperitoneally. Animals were positioned in an animal-holding structure with a cold-light source system. Experimental periodontitis

was induced by applying 5.0 silk ligatures around the second maxillary molars using micro-Castroviejo forceps (Fine Science Tools). Ligatures were maintained for 14 days.

Oral treatment was started two hours before ligature placement and continued daily until the protocol finished. Based on a recent report (23), we fixed the dosage at 10mg/kg for the sEH inhibitor (TPPU), and the EET-mixture was fixed at 1 μg/kg. The combination group utilizes the dosages cited above, concomitantly. On day 14, mice were euthanized, and the presence of ligature was confirmed before sample collection (lymph nodes, blood, and maxillae). Figure 1a represents a flowchart summarizing the experimental design.

Bone Parameter Assessment

Bone parameters were determined after methylene blue staining of defleshed jaws and Micro-CT. Dermestid beetles eliminated the soft tissue from the maxilla samples. The maxilla samples were then submerged in 10% H_2O_2 overnight and rinsed with distilled water the day after. Samples dried for 6 hours and then stained with methylene blue using a microbrush (KG Sorensen) to avoid excessive dye. Images were taken under a microscope (0.63 X10 magnification; Axio observer A1, ZEISS) using AxioVision 4.8 software. The areas between the alveolar bone crest and cementoenamel junction (CEJ) on the palatal side of each maxillary molar were measured using Fiji software (ImageJ).

Maxillae were scanned with a μCT40.Scanco (Medical AG, Bassersdorf, Switzerland) using the parameters: 70kV, 114 μA, and 8.0μm^3 voxel size. Images were reconstructed and exported as Digital Imaging and Communications in Medicine (DICOM) files for analysis. The three-dimensional morphometric examination was conducted in CT-Analyzer software® (Bruker, Belgium). A volume of interest (VOI), including the entire alveolar bone surrounding the roots of the second molar, was individually selected for all samples. The bone within the VOI was segmented using an automatic thresholding algorithm (Figure 2a and b). Bone morphometric indices were calculated in 3D to compare the quantity and structural properties of the trabecular network of the groups. The parameters assessed were bone volume fraction (BV/TV in %), total porosity percentage (Po[tot] in %), bone surface density (BS/TV in %) and trabecular thickness (Tb.Th in mm), trabecular number (Tb.N in 1/mm), trabecular separation (Tb.Sp in mm).

Lipidomic (LM-SPM metabolipidomics)

For blood collection, animals were euthanized by terminal anesthesia, followed by cervical dislocation as a confirmation method. Blood samples were obtained from the left ventricle by performing a thoracotomy. Blood samples were centrifuged at 2000g for 10 minutes at −4C. The serum was collected and stored in a −80 °C freezer until metabolipidomic analysis. LM-SPM metabololipidomics was conducted at the Lipidomics Core Facility, Wayne State University (Detroit, MI, USA), for quantitative analysis of SPM levels and other LMs (27; for detailed information). BCA Assay determined protein concentration to normalize the LM data.

Gene expression quantification

Cervical lymph nodes that drain periodontal tissues were extracted and conditioned in RNAlater solution (Life Technologies). Glassware was used to grind and homogenize the samples in 1 ml of Trizol (Invitrogen). Subsequently, the soluble fraction was incubated for 10 min at 4°C, and 200 μl of chloroform was pipette and incubated for an additional 10 min at 4°C. Samples were then centrifuged at 12,000 g for 20 min, the aqueous phase was collected, and the total RNA was precipitated in 500 μl of isopropyl alcohol for 30 min. At the end of 30 minutes, all samples were centrifuged at 12,000 g for 20 min at 4°C, and the RNA precipitate was washed once with 1 ml 75% ethanol. The purified RNA samples were resuspended in 30 μl of RNase-free water. A total of 1 μg of RNA was used for cDNA synthesis using the reverse transcription kit (SuperScript III, Invitrogen). The cDNA amplification (50 ng) was performed using TaqMan™ Fast Advanced Master Mix (Thermo Fisher). All TaqMan probes of genes quantified and investigated in this study were purchased from Thermo Fisher (Supplementary Table 1). The data are presented as a fold-change of relative quantity using the $2^{-\Delta\Delta Ct}$ method, and β-actin was used as the reference gene.

Flow Cytometry

Cervical lymph nodes were extracted and placed in a falcon tube containing RPMI-1640 (Gibco) + 1% penicillin-streptomycin (Sigma). Single-cell suspensions were obtained by dissociating the samples against 70 μm cell strainers (Sigma-Aldrich) and rinsing them with phosphate-buffered saline (PBS) containing 5% fetal bovine serum (FBS). For cytokine staining, $2x10^6$ cells were incubated for 4h in RPMI −1640 supplemented with 10% FBS, 1% penicillin–streptomycin, Brefeldin A (eBioscience), 50 ng/ml PMA (Sigma), and 1 μg/ml Ionomycin (Sigma). Cells were washed with PBS and stained with the Zombie UV™ Fixable Viability Kit (BioLegend) for 30 min without light. The extracellular staining was conducted in PBS containing 5% FBS, using anti-CD4 (GK1.5, Biolegend) for 30 min at 4°C without light. The intracellular staining was accomplished using a Fixation/Permeabilization staining kit following the manufacturer instructions (eBioscience) and using the following antibodies: anti-Foxp3 (MF-14, Biolegend), Rorγt (Q21-559, eBioscience), and IL-17A (9B10, Biolegend). Cells were analyzed on a BD FACSCanto cytometer (BD Biosciences) using a sequential gating strategy according to the FSC/SSC and SSC/SSC parameters, live/dead staining, and CD4 marker. Data analysis was completed using the FlowJo software (version 10.6.2).

Observational clinical study approval, sample size estimation, and clinical examination.

This study was approved by the Ethics Committee of São Leopoldo Mandic, Campinas, Brazil (CAAE: 50077821.0.0000.5374). Sixteen subjects were selected from the Periodontology Clinic of Faculdade São Leopoldo Mandic, Campinas, Brazil. All admitted subjects signed informed consent. It was an observational clinical study to estimate the expression and levels of sEH in human gingival tissue in healthy and inflamed tissues. A sample of gingival tissue was biopsied. The sample size estimation was established as n=8 per group, totaling 16 subjects, in accordance with previous publications that had the identical purpose of evaluating the expression of different markers in periodontal tissue (28).

Systemically healthy subjects without periodontitis (healthy; n=8) and systemically healthy subjects with periodontitis (inflamed; n=8) were picked from the population referred to the Periodontology Clinic of Faculdade São Leopoldo Mandic (Campinas, Brazil). The inclusion criteria for the healthy group included individuals aged 18 years or older with at least 15 teeth, excluding third molars. Subjects who underwent periodontal surgery for aesthetic purposes were selected (gingivoplasty, for instance). Pregnant or breastfeeding women were excluded, as were smokers and those with a history of subgingival periodontal treatment in the 6 months before the study began. Likewise, individuals continually using mouth rinses containing antimicrobials in the previous 2 months, usage of antibiotics in the preceding 6 months, and long-term use of anti-inflammatory, immunosuppressive, or antiresorptive agents, hormone replacement therapy, and orthodontic treatment were also excluded.

Inclusion criteria for the periodontitis group include subjects with generalized stage 3 or 4, grade C (29), meaning more than 30% of sites presenting probing depth (PD) and clinical attachment level (CAL) ≥ 4 mm with bleeding on probing (BoP), ≥ 6 teeth with ≥1 sites with PD and CAL ≥ 5 mm and BoP, ≥ 1 tooth indicated for extraction due to severe periodontitis. To guarantee areas of periodontitis or inflamed tissue, gingival samples were biopsied from a tooth indicated for extraction due to severe periodontitis (PD and CAL ≥ 7 mm, BoP, mobility and/or bone loss compromising more than 50% of the root).

In clinical examination, the plaque index (PI), PD (mm), BoP, and CAL (mm) were examined at six sites per tooth using a manual periodontal probe (UNC15; Hu-Friedy, Chicago, USA) by the same calibrated examinator (30). All samples biopsied contained junctional and sulcular epithelium and connective tissue. Immediately after gingival collection, samples were stored at −80°C until further processing.

Protein extraction and sEH expression

Gingival samples were prepared in 500μl of Ripa Lysis Buffer (Thermo Scientific), containing protease inhibitor (1:1000; Sigma-Aldrich) and homogenized using a FastPrep-24 Homogenizer (BenchMark Scientific, Sayreville, NJ, USA). Samples were centrifuged for 10 min at 10,000g at 4°C and the supernatants collected and stored at −20 °C. Total protein was measured with the Micro BCA Protein Assay Kit (Thermo Scientific).

A total amount of 30 μg of protein per sample was resolved in a 10% polyacrylamide gel and sequentially transferred onto nitrocellulose membranes (Bio-Rad, Hercules, CA, USA). Membranes were blocked in TBST 5% non-fat milk for 2 hours. Then, the membranes were washed six times in TBST and incubated overnight at 4°C with specific primary antibodies against sEH (a kind gift from Dr. Hammock at the University of California Davis). The membranes were then washed and incubated with specific secondary IgG peroxidase-conjugated antibody (Vector Laboratories, Burlingame, CA, USA) for 1 hour. The membranes were washed, and the protein bands were visualized using ECL solution for 3 minutes (enhanced chemiluminescence; Pierce) and the digital image was acquired using a CCD camera imaging for chemiluminescence (Image Quant LAS 4000 mini, GE Healthcare Life Sciences, Pittsburgh, PA). The Image J software (National Institutes of

Health, Bethesda, MD) was used to measure the bands' optical density (OD). Data are normalized against those of the corresponding GAPDH.

Enzyme-Linked Immunosorbent Assay (ELISA) for sEH

The gingival levels of sEH were assessed using an ultrasensitive PolyHRP-based immunoassay, designed in-house (kindly provided by Dr. Hammock's lab) and described and validated elsewhere (31). A high-binding microplate was coated with anti-human sEH rabbit serum (1:2000 dilution) in carbonate-bicarbonate buffer (100 μL/well) overnight at 4°C on a plate shaker. On the day after, the wells were washed with PBS-0.05%Tween (PBST) and blocked with 3% skim milk in PBS (300μL/well) for 1 hour. During this time, serial concentrations of human sEH standards were prepared in PBS containing 0.1 mg/mL bovine serum albumin. Samples were diluted in a 1:10 ratio. After washing, samples and standards were pipette (100 μL/well) and incubated for 2 hours at room temperature on a plate shaker. Subsequently, biotinylated nanobodies selected for reaction with the human sEH (1 μg/mL, 100 μL/well) in PBS were added to each well after the washing step and incubated for 2 hours. After washing, SA-PolyHRP in PBS (25 ng/mL, 100 μL/well) was added and incubated for another 30 min. After the last washing, the TMB substrate (BD OptEIA™) was pipette (100 μL/well), and the microplate was incubated for 15 minutes, and then stop solution (2 M of sulfuric acid; 100 μL/well) was added. The optical density was reading at 450 nm.

Data analysis

Data were analyzed using Graph Pad Prism software (version 9.5.0). The metabolomic analysis was conducted using the integrated web-based platform MetaboAnalyst (32). The normality of data distribution was determined using the Shapiro–Wilk test. Unpaired -Student t-test was used to determine differences between two experimental groups. One-way analysis of variance (ANOVA) was used when more than two groups were compared, followed by Tukey's post hoc test for multiple comparisons. All data are presented as mean ± SEM. A P-value lower than 0.05 was considered significant.

RESULTS

Modulation of sEH/EET axis restrains alveolar bone resorption during experimental periodontitis in mice.

Initially, we attempted to explore the bone loss prevention capability of the sEHi in the periodontal disease context in mice. We first analyzed the bone loss area in a macroscopic view, using methylene blue stain (Fig. 1b). We demonstrate that pharmacological sEHi (TPPU; 10 mg/kg) prevented alveolar bone loss induced by experimental periodontitis (Fig. 1c). The EET-mix (1 μg/kg) treatments did not restrain bone resorption, which was equivalent to the periodontal disease group (Fig. 1c). Despite inhibiting alveolar bone resorption (Fig. 1c), the combined treatment (sEHi + EET-mix) did not exhibit synergistic actions.

Inasmuch as soluble epoxy hydrolase inhibition prevented bone loss in periodontitis, we sought to investigate the bone microstructure in greater detail. Computed microtomography

(μCT) analyses were performed to assess the quality of the maxillae bone microstructure (Fig. 2). Our data reveal that the experimental periodontitis (PD) group exhibited a noteworthy reduction in bone volume (BV/TV) (Fig. 2c), a decrease in structure complexity (lower BS/TV; Fig. 2d), with a decrease in trabecular thickness (Tb. Th; Fig. 2f) and larger medullary spaces (larger Tb. SP and Tot. Po; Fig. 2g and e) in comparison with the naïve group. No differences were found in the number of bone trabeculae (Tb.N). In control animals (no PD), sEHi maintained bone density (BV/TV) (Fig. 2c), porosity (Tot. Po; Fig. 2e), bone structure complexity (BS/TV; Fig. 2d), and trabecular thickness (Tb. Th; Fig. 2f), whereas there was a significant increase in medullary spaces (Tb.Sp) in the sEHi to the control group (Tb. Sp; Fig. 2g). In periodontal disease animals, the sEHi group exhibited higher bone density and trabecular thickness (Fig. 2b and f), accompanied by lowered porosity (Tot.Po) and smaller medullary spaces (Tb.Sp) (Fig. 2e and g). There were no changes in the trabecular number and bone structure complexity (BS/TV) (Fig. 2h and d). Likewise, the combination treatment (sEHi + EET-mix) demonstrated similar results to sEHi solely in the evaluated parameters. Likened to the control group, the combination group exhibited no changes in bone density (Fig. 2c) and structural complexity (BS/TV) (Fig. 2d). Moreover, there was preservation of trabecular number and thickness (Fig. 2f and h); however, a significant increase in trabecular separation was noted (Fig. 2g), with significantly augmented bone volume (Fig. 2c), greater complexity (BS/TV) (Fig. 2d), and trabecular thickness (Fig. 2f) than periodontal disease, with a lessening in medullary spaces (Tb. Sp and Tot. Po; Fig. 2g and e). Ultimately, EET-mix treatment showed similar bone volume (BV/TV), structure complexity (BS/TV), trabecular number (Tb.N) and thickness (Tb.Th), and porosity to periodontal disease. However, there was a significant increase in trabecular separation. Overall, the inhibition of the sEH enzyme maintained bone parameters comparable to the control group, indicating that sEH inhibition is a potential target for osteolytic inflammatory disorders.

sEHi restrains the impairment of systemic SPMs levels.

It was recently reported that inhibition of sEH augments SPMs levels in mouse saliva (23). Nevertheless, it is now established that periodontal disease is not merely a local condition but rather changes inflammatory parameters systemically (33; 34). In addition, local periodontal inflammation also impacts other conditions, such as diabetes (35), rheumatoid arthritis and osteoarthritis (36; 37; 38), Alzheimer's (39), diseases of the digestive tract (40), and increases the risk of cardiovascular diseases (41; 42).

Considering these findings, we hypothesized that blocking sEH activity would enhance the metabolization of SPMs and other EpFAs from ω-3 and ω-6, boosting their synthesis and bioavailability in the blood serum (Fig. 3). Overall, the data revealed that inhibiting sEH induces the production of SPMs and other intermediary lipid mediators of the SPM cascade (Fig. 3c and d). Interestingly, in the Partial Least Square Discriminant Analysis (PLS-DA), we observed that the lipid profile of SPMs in the sEHi-group tends to be identical to the control group (without disease) (Fig. 3a and b). Furthermore, the sEHi-group differs from the periodontitis group (Fig. 3a and b), portraying the ability of the sEH inhibitors to restrain the development and progression of experimental periodontitis via the production of SPMs. In the Variable Importance in Projection (VIP) score, we can highlight that LXB_4,

RvD6, and 11-HETE exhibit high scores in the sEHi-group (Fig. 3c), and in the heatmap with clustering analysis, an exclusive cluster is formed with sham and sEHi-group (Fig. 3d), endorsing the PLS-DA findings. Lastly, we totaled the SPMs per group (Fig. 3e) and found that sEHi treatment restrained the impairment of SPM production in experimental periodontitis.

Univariate analysis was carried out (Figs. 4 and 5), according to the polyunsaturated fatty acids (PUFAs) pathway involved. Notably, in the lipoxin formation pathway derived from ω6 arachidonic acid (Fig. 4), pharmacological sEHi increases serum levels of 11-HETE (Fig. 4a), 12(S)-HHTrE (Fig. 4b), 5(S), 12(S)-DiHETE (Fig. 4c), LXA_4 (Fig. 4e), and LXB_4 (Fig. 4f). These findings demonstrate that sEHi favors the synthesis of SPMs (e.g., LXA_4 and LXB_4) and their intermediate metabolites, overseeing the resolution of the inflammatory process. As for the classic mediators of inflammation, sEHi augmented the systemic levels of PGE_2 (Fig. 4h) and $PGF_{2\alpha}$ (Fig. 4i).

Regarding eicosapentaenoic acid (EPA), docosahexaenoic acid (DHA), and docosapentaenoic acid (DPA) derivatives from ω3 (Fig. 5), sEHi amplified the levels of 5(S),15(S)-DiHEPE (Fig. 5b), RvE2 and RvD6 (Fig. 5c and g). Nonetheless, maresin1 and RvD1 exhibited lower values in the sEHi and combination groups (Fig. 5d and e). In both cases, it is plausible to suggest that sEH inhibition stimulates the synthesis of lipid mediators through 5-LOX and 12-LOX in different PUFAs as substrates, which are associated pathways with the SPMs and other mediator synthesis, which feature high resolving capacity. Furthermore, the metabolites generated by the 5-LOX and 12-LOX regulate the classical mediators of inflammation through an antagonistic function (decreasing their production) or acting synergistically and altering their immune system response pattern. Overall, the pharmacological inhibition of sEH induces the lipid mediator class switch promoting SPM production, like LXA_4, LXB_4, RvE2, and RvD6, at bioactive levels (43).

The sEH/EETs axis affects Treg/Th17 ratio in experimental periodontitis.

Although distinct T-cell phenotypes have already been identified (Th1, Th2, Th9, Th17, Th22, and Treg) (44), Th17 and Treg balance is essential in the pathogenesis of periodontal disease. They can be divided simply into two axes: *a)* inflammatory and osteoclastogenic axis, where the Th17 lymphocyte dominates, and *b)* healing axis that mechanistically prevents the disease and its progression, comprising Treg lymphocytes (45). Considering that the inhibition of sEH augments the SPM levels systemically and assuming the critical role that T-cells play in the pathogenesis of periodontitis, we decided to scrutinize the balance between Th17/Treg in the cervical lymph nodes through Flow Cytometry (Fig. 6), transcription factors and target genes (Fig.7).

To effectively identify the distinct subpopulations of lymphocytes, the following workflow was applied: ***1)*** data was cleaned by manually excluding doublets, debris, and dead cells; ***2)*** The gating strategy for CD4+ cells was applied; ***3)*** Then, intracellular labeling was performed for FOXP3+, or IL17+, or $ROR\gamma t^+$ cells; ***4)*** distinct cell populations were analyzed, and phenotypes identified (4). Total cell counting from the cervical lymph node exhibited increased cells in the experimental periodontitis. Treatment with EETs reduced these cell counts, while sEHi and the combination treatment did not (Fig. 6b). Regarding the

percentage of $CD4^+$ cells, there was no difference among the groups (Fig. 6c). On the other hand, sEH inhibition and the combination raised the percentage of $CD4^+FOXP3^+$ cells and decreased the percentage of $CD4^+IL17^+$ cells (Fig. 6d and e). The Treg/Th17 ratio confirms that the modulation of the sEH/EET axis impacts the T-cell profile, favoring Treg subtypes (Fig. 6g).

Similarly, we examined key cytokines and transcription factors for Th17 and Treg profiles by mRNA expression. Corroborating the FC data, we showed that the sEHi augments the gene expression of Foxp3, Ctl4, and Tgfβ1 (Fig. 7b - d), exhibiting the polarization of these lymphocytes towards the Treg profile. Furthermore, Rorγt, Il17a, and Il23a gene expression were reduced with sEHi and combination (Fig. 7e - g), indicating fewer Th17 cells in cervical lymph nodes. Therefore, we demonstrate that the pharmacological inhibition of sEH and its association with EETs favors a positive balance between Treg/Th17, indicating less activation of inflammatory profiles and hindering the progression of periodontal disease.

Inflamed gingival tissue presents higher sEH expression and levels.

Finally, looking toward future clinical applicability and translation, we collected samples of healthy gingiva (patients with indication for gingivoplasty) and inflamed tissues from patients classified in grade C, stages III and IV (gingival tissues removed from exodontia procedure), and measured the protein levels and expression of the sEH enzyme (Fig. 8a). The demographic features and periodontal parameters of the participants are included in Table 1. Patients with inflamed gingival tissue showed increased expression and protein levels of sEH when compared to healthy patients (Fig. 8b and c). Additionally, we found a positive correlation with higher levels of sEH and clinical parameters of periodontitis, such as probing depth and clinical attachment loss (Fig. 8d). Therefore, these findings indicate the presence of sEH is associated with periodontal disease severity.

DISCUSSION

In the present study, we report that pharmacological inhibition of sEH prevents the development of experimental periodontitis and maintains bone architecture and density. Overall, the pharmacological inhibition of sEH prevents bone resorption and maintains bone quality. Additionally, sEHi restrains the impairment in SPM production induced by experimental periodontitis, mainly by stimulating the synthesis of LXA_4, LXB_4, RvE2, and RvD6. Immunologically, we found a higher percentage of regulatory T-cells than Th17 in the sEHi-group, associated with augmented mRNA expression of Treg markers, like *Foxp3*, *Ctla4*, and *Tgfb1*. Finally, in patients with periodontitis grade C, stages III and IV, higher levels and expression of sEH were found and are correlated with increased probing depth and clinical attachment loss. Thus, the modulation of sEH/EETs favors the resolution pathways of inflammation through SPM production, avoiding exaggerated immune response and destruction of hard tissue. A positive correlation between sEH and periodontal clinical parameters indicates involvement in disease severity.

These actions are somewhat justified by the association between pharmacological sEH inhibition and higher SPMs systemically, mainly LXA_4, LXB_4, RvE2, and RvD6. When total SPMs are analyzed, sEH inhibition restrains the impairment evoked by experimental

periodontitis and re-establishes physiological levels of SPMs protecting the periodontium from destruction. In cervical lymph nodes, we found that modulating the sEH/EET axis directly impacts the T-cell profile and Th17/Treg balance, favoring Treg subtypes. Last but not least, we uncover for the first time in human gingival tissue increased levels and expression of sEH in patients with periodontitis (grade C and stages III and IV). In addition, these levels correlate with worse clinical parameters of periodontal disease, such as probing depth and clinical attachment loss, suggesting an association with sEH in the gingival tissue and periodontal disease pathology and severity.

Using the ligature-induced model of experimental periodontitis, we reported here that pharmacological inhibition of sEH prevented bone resorption. Looking more deeply into bone parameters with micro-CT assessed bone morphology and microarchitecture revealed that sEHi maintains bone volume and density, trabecular thickness, and separation. Furthermore, sEHi reduces porosity and trabecular separation, implying that the bone preserved kept its structure and functionality. It has been previously documented that sEHi blocked bone loss in *A. actinomycetemcomitans*-induced periodontal disease (46; 47) and ligature-induced (23; 48) periodontal disease. Likewise, targeting sEH protects bone morphology in a model of osteonecrosis of the femoral head induced by exposure to tobacco smoke (49). From a regenerative perspective, it was recently shown that TPPU reversed the release of inflammatory cytokines by human dental pulp stem cells under inflammatory conditions (LPS-induced). It also stimulated osteogenic differentiation by osteogenesis-related genes alkaline phosphatase (*Alp*), osteocalcin (*Ocn*), and runt-related transcription factor 2 (*Runx2*). The researchers have also shown that TPPU decreases alveolar ridge resorption after tooth extraction (50).

Periodontitis is a chronic inflammatory disease that reflects a deficiency in the resolution phase of the acute inflammation, especially by dysregulating the production of resolution lipid mediators, such as specialized pro-resolving mediators (SPMs) (51). For instance, in the gingival tissue of periodontitis patients, elevated levels of SPM biosynthetic pathway markers were found; however, their respective receptors were deficiently expressed (e.g., Leukotriene B_4 receptor 1 (BLT1), associated with resolvin from E-series), compromising the resolution initiation, leading to an exaggerated and destructive inflammatory response in the periodontium (52). Further, the subgingival microbiome correlates with SPMs, SPM pathway markers, and SPM gene receptors (53). Specifically, four *Selenomonas* species and *A. geminatus* (which are not described as periodontopathogens) were highly correlated with several lipid mediators, such as 5(S),12(S)-dihydroxy-6E,8Z,11E,14Z-eicosatetraenoic acid (5(S)12(S)-DiHETE), RvD1, MaR1, and leukotriene B_4 (LTB_4). Additionally, these bacteria are reported to possess enzymes that metabolize linoleic and ALA-derived lipids, which are known to produce resolution bioactive lipids (54). These data suggest that the profile of lipids directly impacts bacterial composition, indicating an interaction among inflammation, lipids, and microbiota.

Here, our data revealed that pharmacological sEHi treated animals exhibits comparable SPM profiles to baseline animals, which differ from the other groups. In addition, sEHi restrains the impairment of SPM levels caused by experimental periodontitis. Notably, LXA_4 and LXB_4 were upregulated, as well as RvE2 and RvD6. It is interesting that

increased levels of LXA_4 and RvE2 were found in the saliva of animals treated with sEHi in experimental periodontitis, as well as their respective receptors in gingival tissue, N-formyl peptide receptor 2 (ALX/FPR2) and Chemerin Receptor 23 (ChemR23/ERV1), respectively (23). Lipoxins were the first SPMs isolated and described by Serhan and colleagues (Serhan et al., 1984) and fostered the resolution phase of inflammation by counteracting excessive leukocyte infiltration, stimulating an increase in efferocytosis activity, and facilitating non-phlogistic recruitment of macrophages (56; 57). In addition, RvE2 and RvD6 were also found to increase systemically. Resolvins from E-series and D-series displayed substantial actions to alleviate inflammation by orchestrating the immune system response, blocking inflammasome and NF-κB signaling and downstream cytokine production, enhancing the clearance of cellular debris, and stimulating phagocytosis (13; 58). Higher levels of prostaglandin E_2, a potent and well-known inflammatory lipid from AA metabolism, were found. Although much is described regarding its inflammatory role, PGE_2 also presents an anti-inflammatory function, depending on where and when it is produced (59; 60). Specifically, PGE_2 is essential for neutrophil inflammation resolution, inducing cell reprogramming to switch from 5-LOX products towards 15-LOX, to produce LXA_4 (61). Thus, pharmacological sEHi stimulates the synthesis of SPMs in blood serum, restraining excessive inflammatory reactions and guiding immune resolution activities.

In chronic inflammatory diseases, such as arthritis and periodontal disease, Th17 cells display destructive features, producing a wide range of pro-inflammatory cytokines, including IL-17, IL-23, IL-22, IL-6, IL-1β, and TNFα (62). In our study, pharmacological sEHi impacts Th17 activation in the cervical lymph nodes. In the arthritis model, sEHi similarly decreased Th17 gene marker expression (*Il17* and *Roryt*) in the knee joint (21). In addition, SPMs like lipoxins and resolvins also prevent Th17 activation and proliferation in murine and rabbit models of periodontitis (4; 63; 64; 65; 66). On the other hand, regulatory T cells (Treg) were boosted in cervical lymph nodes with sEHi therapy. Higher expression of *Foxp3*, *Ctla4*, and *Tfgb1* was seen compared to periodontitis group. Additionally, the Treg/Th17 ratio favors the regulatory profile, leading to the resolution of inflammation. Interestingly, n-3 polyunsaturated acid (PUFA) supplementation (~1053 mg/per day), i.e., α-linolenic (~230 mg), eicosapentaenoic (~15 mg), and docosahexaenoic acid (~105 mg) changes the immune response profile, improving regulatory T-cell profile (67). However, as we know that SPMs can directly impact T-cell differentiation (68), we cannot infer that these findings were due to sEHi effects. These could be an indirect effect mediated by SPMs induced by sEH inhibition. Nonetheless, by controlling Th17 activation and stimulating the regulatory T-cells, bone loss was preserved.

Last, we collected gingival samples from Stages III-IV grade C periodontitis and healthy subjects to investigate the expression and levels of sEH and associate it with the progression of periodontal disease. We are the first to examine the presence of sEH in human gingival tissue. Previously, we showed that a ligature-induced periodontitis model enhanced sEH (*Epxh2*) gene expression (23). In the present study, higher expression, and levels of sEH were found in inflamed gingival tissues compared to non-inflamed tissues. Further, a positive correlation was observed when probing depth, and clinical attachment loss of the sampled teeth was correlated with sEH levels. These data suggest that sEH is associated with periodontal disease and is associated with the severity of periodontitis.

Taken together, the present study demonstrated that sEHi blocked alveolar bone loss and maintained bone density and architecture. Considering that periodontitis induces a systemic low-grade inflammatory response that is a risk factor for several comorbidities, sEHi restrains the impairment of SPM production, and increases levels of LXA_4, LXB_4, RvE2, and RvD6 in serum. In addition, the Th17/Treg ratio favors the regulatory T-cell phenotype in cervical lymph nodes, essential for periodontium integrity and preservation. Remarkably, we showed that sEH levels are associated with the worst cases of periodontal disease, positively correlated with deep periodontal pockets and loss of clinical attachment. Therefore, these data highlight the critical role of sEH in periodontal disease, as in other chronic inflammatory osteolytic diseases.

Supplementary Material

Refer to Web version on PubMed Central for supplementary material.

Acknowledgements

We would like to thank Yoganathan Subbiah for technical support and animal care. We want to acknowledge The Forsyth Institute's Flow cytometry and Micro-CT cores and Forsyth's Animal Facility. We appreciate Qiyi He for preparing the sEH antibody and ELISA kit.

This work was supported in part by USPHS grant DE025020 from NIDCR (to T.V.D.), by São Paulo Research Foundation (FAPESP) grants #2017/22334-9 and #2019/22645-0 (to M.H.N. and H.B.A., respectively), and by the National Institute of Environmental Health Sciences (NIEHS) River Award R35 ES030443-01 and NIEHS Superfund Program P42 ES004699 (to B.D.H.).

Data Availability Statement

The data that support the findings of this study are available from the corresponding author upon reasonable request. Some data may not be made available because of privacy or ethical restrictions.

REFERENCES

1. Eke PI, Dye BA, Wei L, Thornton-Evans GO, Genco RJ. Prevalence of Periodontitis in Adults in the United States: 2009 and 2010. Journal of Dental Research. 2012;91(10):914–920. doi:10.1177/0022034512457373 [PubMed: 22935673]
2. Chen MX, Zhong YJ, Dong QQ, Wong HM, Wen YF. Global, regional, and national burden of severe periodontitis, 1990-2019: An analysis of the Global Burden of Disease Study 2019. J Clin Periodontol. 2021 Sep;48(9):1165–1188. doi: 10.1111/jcpe.13506. [PubMed: 34101223]
3. Bartold PM, Van Dyke TE. Host modulation: controlling the inflammation to control the infection. Periodontol 2000. 2017 Oct;75(1):317–329. doi: 10.1111/prd.12169. [PubMed: 28758299]
4. Alvarez C, Abdalla H, Sulliman S, Rojas P, Wu YC, Almarhoumi R, Huang RY, Galindo M, Vernal R, Kantarci A. RvE1 Impacts the Gingival Inflammatory Infiltrate by Inhibiting the T Cell Response in Experimental Periodontitis. Front Immunol. 2021 May 3; 12:664756. doi: 10.3389/fimmu.2021.664756. [PubMed: 34012448]
5. Ikeuchi T, Moutsopoulos NM. Osteoimmunology in periodontitis; a paradigm for Th17/IL-17 inflammatory bone loss. Bone. 2022 Oct; 163:116500. doi: 10.1016/j.bone.2022.116500. [PubMed: 35870792]
6. Matthews JB, Wright HJ, Roberts A, Ling-Mountford N, Cooper PR, Chapple ILC. Neutrophil Hyper-responsiveness in Periodontitis. Journal of Dental Research. 2007;86(8):718–722. doi:10.1177/154405910708600806 [PubMed: 17652198]

7. White PC, Chicca IJ, Cooper PR, Milward MR, Chapple ILC. Neutrophil Extracellular Traps in Periodontitis: A Web of Intrigue. Journal of Dental Research. 2016;95(1):26–34. doi:10.1177/0022034515609097 [PubMed: 26442948]
8. Alvarez C, Suliman S, Almarhoumi R, Vega ME, Rojas C, Monasterio G, Galindo M, Vernal R, Kantarci A. Regulatory T cell phenotype and anti-osteoclastogenic function in experimental periodontitis. Sci Rep. 2020 Nov 4;10(1):19018. doi: 10.1038/s41598-020-76038-w. [PubMed: 33149125]
9. Deng J, Lu C, Zhao Q, Chen K, Ma S, Li Z. The Th17/Treg cell balance: crosstalk among the immune system, bone and microbes in periodontitis. J Periodontal Res. 2022 Apr;57(2):246–255. doi: 10.1111/jre.12958. [PubMed: 34878170]
10. Levy BD, Clish CB, Schmidt B, Gronert K, Serhan CN. Lipid mediator class switching during acute inflammation: signals in resolution. Nat Immunol. 2001 Jul;2(7):612–9. doi: 10.1038/89759. [PubMed: 11429545]
11. Serhan CN. Lipoxins and aspirin-triggered 15-epi-lipoxins are the first lipid mediators of endogenous anti-inflammation and resolution. Prostaglandins Leukot Essent Fatty Acids. 2005 Sep-Oct;73(3-4):141–62. doi: 10.1016/j.plefa.2005.05.002. [PubMed: 16005201]
12. Serhan CN, Chiang N, Van Dyke TE. Resolving inflammation: dual anti-inflammatory and pro-resolution lipid mediators. Nat Rev Immunol. 2008 May;8(5):349–61. doi: 10.1038/nri2294. [PubMed: 18437155]
13. Eltay EG, Van Dyke T. Resolution of inflammation in oral diseases. Pharmacol Ther. 2023 Jul; 247:108453. doi: 10.1016/j.pharmthera.2023.108453. [PubMed: 37244405]
14. Serhan CN. Pro-resolving lipid mediators are leads for resolution physiology. Nature. (2014) 510(7503):92–101. doi: 10.1038/nature13479 [PubMed: 24899309]
15. Haeggström JZ, Funk CD. Lipoxygenase and leukotriene pathways: biochemistry, biology, and roles in disease. Chem Rev. (2011) 111(10):5866–98. doi: 10.1021/cr200246d [PubMed: 21936577]
16. Hoxha M, Zappacosta B. CYP-derived eicosanoids: implications for rheumatoid arthritis. Prostaglandins Other Lipid Mediat. (2020) 146:106405. doi: 10.1016/j.prostaglandins.2019.106405 [PubMed: 31838196]
17. Hammock BD, Wang W, Gilligan MM, Panigrahy D. Eicosanoids: the overlooked storm in coronavirus disease 2019 (COVID-19)? Am J Pathol. (2020) 190(9):1782–8. doi: 10.1016/j.ajpath.2020.06.010 [PubMed: 32650004]
18. Wang Y, Wagner KM, Morisseau C, Hammock BD. Inhibition of the Soluble Epoxide Hydrolase as an Analgesic Strategy: A Review of Preclinical Evidence. J Pain Res. 2021 Jan 13; 14:61–72. doi: 10.2147/JPR.S241893. [PubMed: 33488116]
19. Kodani SD, Hammock BD. The 2014 bernard B. Brodie award lecture-epoxide hydrolases: drug metabolism to therapeutics for chronic pain. Drug Metab Dispos. (2015) 43(5):788–802. doi: 10.1124/dmd.115.063339 [PubMed: 25762541]
20. Norwood S, Liao J, Hammock BD, Yang GY. Epoxyeicosatrienoic acids and soluble epoxide hydrolase: potential therapeutic targets for inflammation and its induced carcinogenesis. Am J Transl Res. (2010) 2(4):447–57. [PubMed: 20733953]
21. Trindade-da-Silva CA, Clemente-Napimoga JT, Abdalla HB, Rosa SM, Ueira-Vieira C, Morisseau C, Verri WA Jr, Montalli VAM, Hammock BD, Napimoga MH. Soluble epoxide hydrolase inhibitor, TPPU, increases regulatory T cells pathway in an arthritis model. FASEB J. 2020 Jul;34(7):9074–9086. doi: 10.1096/fj.202000415R. [PubMed: 32400048]
22. Abdalla HB, Napimoga MH, Teixeira JM, Trindade-da-Silva CA, Pieroni VL, Dos Santos Araújo FSM, et al. Soluble epoxide hydrolase inhibition avoid formalin-induced inflammatory hyperalgesia in the temporomandibular joint. Inflammopharmacology. (2022) 30(3):981–90. doi: 10.1007/s10787-022-00965-5 [PubMed: 35303234]
23. Abdalla HB, Alvarez C, Wu YC, Rojas P, Hammock BD, Maddipati KR, Trindade-da-Silva CA, Soares MQS, Clemente-Napimoga JT, Kantarci A, Napimoga MH, Van Dyke TE. Soluble epoxide hydrolase inhibition enhances production of specialized pro-resolving lipid mediator and promotes macrophage plasticity. Br J Pharmacol. 2023 Jun;180(12):1597–1615. doi: 10.1111/bph.16009. [PubMed: 36508312]

24. Rose TE, Morisseau C, Liu JY, Inceoglu B, Jones PD, Sanborn JR, Hammock BD. 1-Aryl-3-(1-acylpiperidin-4-yl)urea inhibitors of human and murine soluble epoxide hydrolase: structure-activity relationships, pharmacokinetics, and reduction of inflammatory pain. J Med Chem. 2010 Oct 14;53(19):7067–75. [PubMed: 20812725]

25. Morisseau C, Inceoglu B, Schmelzer K, Tsai HJ, Jinks SL, Hegedus CM, Hammock BD. Naturally occurring monoepoxides of eicosapentaenoic acid and docosahexaenoic acid are bioactive antihyperalgesic lipids. J Lipid Res. 2010 Dec;51(12):3481–90. [PubMed: 20664072]

26. Kilkenny C, Browne W, Cuthill IC, Emerson M, Altman DG, & Group NCRRGW (2010). Animal research: Reporting in vivo experiments: The ARRIVE guidelines. British Journal of Pharmacology, 160(7), 1577–1579. [PubMed: 20649561]

27. Maddipati KR, Romero R, Chaiworapongsa T, Zhou SL, Xu Z, Tarca AL, Kusanovic JP, Munoz H, Honn KV. Eicosanomic profiling reveals dominance of the epoxygenase pathway in human amniotic fluid at term in spontaneous labor. FASEB J. 2014 Nov;28(11):4835–46. doi: 10.1096/fj.14-254383. [PubMed: 25059230]

28. Zhang Q, Liu J, Ma L, Bai N, Xu H. Wnt5a is involved in LOX-1 and TLR4 induced host inflammatory response in peri-implantitis. J Periodontal Res. 2020 Apr;55(2):199–208. [PubMed: 31593304]

29. Papapanou PN, Sanz M, Buduneli N, Dietrich T, Feres M, Fine DH, Flemmig TF, Garcia R, Giannobile WV, Graziani F, Greenwell H, Herrera D, Kao RT, Kebschull M, Kinane DF, Kirkwood KL, Kocher T, Kornman KS, Kumar PS, Loos BG, Machtei E, Meng H, Mombelli A, Needleman I, Offenbacher S, Seymour GJ, Teles R, Tonetti MS. Periodontitis: Consensus report of workgroup 2 of the 2017 World Workshop on the Classification of Periodontal and Peri-Implant Diseases and Conditions. J Periodontol. 2018 Jun;89 Suppl 1: S173–S182. doi: 10.1002/JPER.17-0721. [PubMed: 29926951]

30. Araujo MW, Hovey KM, Benedek JR, Grossi SG, Dorn J, Wactawski-Wende J, Genco RJ, Trevisan M. Reproducibility of probing depth measurement using a constant-force electronic probe: analysis of inter- and intraexaminer variability. J Periodontol. 2003 Dec;74(12):1736–40. doi: 10.1902/jop.2003.74.12.1736.

31. Li D, Cui Y, Morisseau C, Gee SJ, Bever CS, Liu X, Wu J, Hammock BD, Ying Y. Nanobody Based Immunoassay for Human Soluble Epoxide Hydrolase Detection Using Polymeric Horseradish Peroxidase (PolyHRP) for Signal Enhancement: The Rediscovery of PolyHRP? Anal Chem. 2017 Jun 6;89(11):6248–6256. doi: 10.1021/acs.analchem.7b01247. [PubMed: 28460522]

32. Xia J, Wishart DS. Web-based inference of biological patterns, functions and pathways from metabolomic data using MetaboAnalyst. Nat Protoc. 2011 Jun;6(6):743–60. doi: 10.1038/nprot.2011.319. [PubMed: 21637195]

33. Genco RJ, Sanz M. Clinical and public health implications of periodontal and systemic diseases: An overview. Periodontol 2000. 83(1):7–13 (2020). [PubMed: 32385880]

34. Hajishengallis G, Chavakis T. Local and systemic mechanisms linking periodontal disease and inflammatory comorbidities. Nat Rev Immunol. 21(7):426–440 (2021). [PubMed: 33510490]

35. D'Aiuto F, Gkranias N, Bhowruth D, Khan T, Orlandi M, Suvan J, Masi S, Tsakos G, Hurel S, Hingorani AD, Donos N, Deanfield JE; TASTE Group. Systemic effects of periodontitis treatment in patients with type 2 diabetes: a 12 month, single-centre, investigator-masked, randomised trial. Lancet Diabetes Endocrinol. 2018 Dec;6(12):954–965. doi: 10.1016/S2213-8587(18)30038-X. [PubMed: 30472992]

36. Ortiz P, Bissada NF, Palomo L, Han YW, Al-Zahrani MS, Panneerselvam A, Askari A. Periodontal therapy reduces the severity of active rheumatoid arthritis in patients treated with or without tumor necrosis factor inhibitors. J Periodontol. 2009 Apr;80(4):535–40. doi: 10.1902/jop.2009.080447. [PubMed: 19335072]

37. Hashimoto M, Yamazaki T, Hamaguchi M, Morimoto T, Yamori M, Asai K, Isobe Y, Furu M, Ito H, Fujii T, Terao C, Mori M, Matsuo T, Yoshitomi H, Yamamoto K, Yamamoto W, Bessho K, Mimori T. Periodontitis and Porphyromonas gingivalis in preclinical stage of arthritis patients. PLoS One. 2015 Apr 7;10(4):e0122121. doi: 10.1371/journal.pone.0122121. [PubMed: 25849461]

38. Ma KS, Lai JN, Thota E, Yip HT, Chin NC, Wei JC, Van Dyke TE. Bidirectional Relationship Between Osteoarthritis and Periodontitis: A Population-Based Cohort Study Over a 15-year

Follow-Up. Front Immunol. 2022 Jul 25;13:909783. doi: 10.3389/fimmu.2022.909783. [PubMed: 35958545]

39. Kantarci A, Tognoni CM, Yaghmoor W, Marghalani A, Stephens D, Ahn JY, Carreras I, Dedeoglu A. Microglial response to experimental periodontitis in a murine model of Alzheimer's disease. Sci Rep. 2020 Oct 29;10(1):18561. doi: 10.1038/s41598-020-75517-4. [PubMed: 33122702]
40. Kitamoto S, Nagao-Kitamoto H, Jiao Y, Gillilland MG 3rd, Hayashi A, Imai J, Sugihara K, Miyoshi M, Brazil JC, Kuffa P, Hill BD, Rizvi SM, Wen F, Bishu S, Inohara N, Eaton KA, Nusrat A, Lei YL, Giannobile WV, Kamada N. The Intermucosal Connection between the Mouth and Gut in Commensal Pathobiont-Driven Colitis. Cell. 2020 Jul 23;182(2):447–462.e14. doi: 10.1016/j.cell.2020.05.048. [PubMed: 32758418]
41. Schenkein HA, Papapanou PN, Genco R, Sanz M. Mechanisms underlying the association between periodontitis and atherosclerotic disease. Periodontol 2000. 83(1):90–106 (2020). [PubMed: 32385879]
42. Panezai J, Ghaffar A, Altamash M, Åberg M, Van Dyke TE, Larsson A, Engström PE. Periodontal Disease Augments Cardiovascular Disease Risk Biomarkers in Rheumatoid Arthritis. Biomedicines. 2022 Mar 19;10(3):714. doi: 10.3390/biomedicines10030714. [PubMed: 35327515]
43. Norris PC, Serhan CN. Metabololipidomic profiling of functional immunoresolvent clusters and eicosanoids in mammalian tissues. Biochem Biophys Res Commun. 2018 Oct 7;504(3):553–561. doi: 10.1016/j.bbrc.2018.03.037. [PubMed: 29524409]
44. Bluestone JA, Mackay CR, O'Shea JJ, Stockinger B. The functional plasticity of T cell subsets. Nat Rev Immunol. 2009 Nov;9(11):811–6. doi: 10.1038/nri2654. [PubMed: 19809471]
45. Garlet GP, Giannobile WV. Macrophages: the bridge between inflammation resolution and tissue repair? J Dental Res. (2018) 97:1079–81. doi:10.1177/0022034518785857
46. Trindade-da-Silva CA, Bettaieb A, Napimoga MH, Lee KSS, Inceoglu B, Ueira-Vieira C, Bruun D, Goswami SK, Haj FG, Hammock BD. Soluble Epoxide Hydrolase Pharmacological Inhibition Decreases Alveolar Bone Loss by Modulating Host Inflammatory Response, RANK-Related Signaling, Endoplasmic Reticulum Stress, and Apoptosis. J Pharmacol Exp Ther. 2017 Jun;361(3):408–416. doi: 10.1124/jpet.116.238113. [PubMed: 28356494]
47. Napimoga MH, Rocha EP, Trindade-da-Silva CA, Demasi APD, Martinez EF, Macedo CG, Abdalla HB, Bettaieb A, Haj FG, Clemente-Napimoga JT, Inceoglu B, Hammock BD. Soluble epoxide hydrolase inhibitor promotes immunomodulation to inhibit bone resorption. J Periodontal Res. 2018 Oct;53(5):743–749. doi: 10.1111/jre.12559. [PubMed: 29851077]
48. Abdalla HB and Van Dyke TE (2023) The impact of the soluble epoxide hydrolase cascade on periodontal tissues. Front. Dent. Med 4:1129371. doi: 10.3389/fdmed.2023.1129371
49. Xu J, Qiu X, Yu G, Ly M, Yang J, Silva RM, Zhang X, Yu M, Wang Y, Hammock B, Pinkerton KE, Zhao D. Soluble epoxide hydrolase inhibitor can protect the femoral head against tobacco smoke exposure-induced osteonecrosis in spontaneously hypertensive rats. Toxicology. 2022 Jan 15; 465:153045. doi: 10.1016/j.tox.2021.153045. [PubMed: 34801612]
50. Dang H, Chen W, Chen L, Huo X, Wang F. TPPU inhibits inflammation-induced excessive autophagy to restore the osteogenic differentiation potential of stem cells and improves alveolar ridge preservation. Sci Rep. 2023 Jan 28;13(1):1574. doi: 10.1038/s41598-023-28710-0. [PubMed: 36709403]
51. Panezai J, Van Dyke TE. Resolution of inflammation: Intervention strategies and future applications. Toxicol Appl Pharmacol. 2022 Aug 15; 449:116089. doi: 10.1016/j.taap.2022.116089. [PubMed: 35644268]
52. Ferguson B, Bokka NR, Maddipati KR, Ayilavarapu S, Weltman R, Zhu L, Chen W, Zheng WJ, Angelov N, Van Dyke TE, Lee CT. Distinct Profiles of Specialized Pro-resolving Lipid Mediators and Corresponding Receptor Gene Expression in Periodontal Inflammation. Front Immunol. 2020 Jun 25; 11:1307. doi: 10.3389/fimmu.2020.01307. [PubMed: 32670289]
53. Lee CT and Tribble GD (2023) Roles of specialized pro-resolving mediators and omega-3 polyunsaturated fatty acids in periodontal inflammation and impact on oral microbiota. Front. Oral. Health 4:1217088. doi: 10.3389/froh.2023.1217088 [PubMed: 37559676]
54. Lee CT, Li R, Zhu L, Tribble GD, Zheng WJ, Ferguson B, Maddipati KR, Angelov N, Van Dyke TE. Subgingival Microbiome and Specialized Pro-Resolving Lipid Mediator Pathway Profiles Are

Correlated in Periodontal Inflammation. Front Immunol. 2021 Jun 10; 12:691216. doi: 10.3389/fimmu.2021.691216. [PubMed: 34177951]

55. Serhan CN, Hamberg M, Samuelsson B. Lipoxins: novel series of biologically active compounds formed from arachidonic acid in human leukocytes. Proc Natl Acad Sci U S A. 1984 Sep;81(17):5335–9. doi: 10.1073/pnas.81.17.5335. [PubMed: 6089195]
56. Godson C, Mitchell S, Harvey K, Petasis NA, Hogg N, & Brady HR (2000). Cutting edge: Lipoxins rapidly stimulate nonphlogistic phagocytosis of apoptotic neutrophils by monocyte-derived macrophages. Journal of Immunology 164(4), 1663–1667. 10.4049/jimmunol.164.4.1663.
57. Serhan CN. Lipoxins and aspirin-triggered 15-epi-lipoxin biosynthesis: an update and role in anti-inflammation and pro-resolution. Prostaglandins Other Lipid Mediat. 2002 Aug;68-69:433–55. doi: 10.1016/s0090-6980(02)00047-3. [PubMed: 12432935]
58. Dalli J, Chiang N, Serhan CN. Elucidation of novel 13-series resolvins that increase with atorvastatin and clear infections. Nat Med. 2015 Sep;21(9):1071–5. doi: 10.1038/nm.3911. [PubMed: 26236990]
59. Scher JU, Pillinger MH. The anti-inflammatory effects of prostaglandins. J Investig Med. 2009 Aug;57(6):703–8. doi: 10.2310/JIM.0b013e31819aaa76.
60. Feng Y, Renshaw S, Martin P. Live imaging of tumor initiation in zebrafish larvae reveals a trophic role for leukocyte-derived PGE_2. Curr Biol. 2012 Jul 10;22(13):1253–9. doi: 10.1016/j.cub.2012.05.010. [PubMed: 22658594]
61. Loynes CA, Lee JA, Robertson AL, Steel MJ, Ellett F, Feng Y, Levy BD, Whyte MKB, Renshaw SA. PGE2 production at sites of tissue injury promotes an anti-inflammatory neutrophil phenotype and determines the outcome of inflammation resolution in vivo. Sci Adv. 2018 Sep 5;4(9):eaar8320. doi: 10.1126/sciadv.aar8320. [PubMed: 30191175]
62. Bettelli E, Korn T, Oukka M, Kuchroo VK. Induction and effector functions of TH17 cells. Nature (2008) 453(7198):1051–7. 10.1038/nature07036. [PubMed: 18563156]
63. Hasturk H, Kantarci A, Ohira T, Arita M, Ebrahimi N, Chiang N, Petasis NA, Levy BD, Serhan CN, Van Dyke TE. RvE1 protects from local inflammation and osteoclast- mediated bone destruction in periodontitis. FASEB J. 2006 Feb;20(2):401–3. doi: 10.1096/fj.05-4724fje. [PubMed: 16373400]
64. Mizraji G, Heyman O, Van Dyke TE, Wilensky A. Resolvin D2 Restrains Th1 Immunity and Prevents Alveolar Bone Loss in Murine Periodontitis. Front Immunol. 2018 Apr 25; 9:785. doi: 10.3389/fimmu.2018.00785. [PubMed: 29922275]
65. Oner F, Alvarez C, Yaghmoor W, Stephens D, Hasturk H, Firatli E, Kantarci A. Resolvin E1 Regulates Th17 Function and T Cell Activation. Front Immunol. 2021 Mar 17; 12:637983. doi: 10.3389/fimmu.2021.637983. [PubMed: 33815391]
66. Yamada H, Saegusa J, Sendo S, Ueda Y, Okano T, Shinohara M, Morinobu A. Effect of resolvin D5 on T cell differentiation and osteoclastogenesis analyzed by lipid mediator profiling in the experimental arthritis. Sci Rep. 2021 Aug 27;11(1):17312. doi: 10.1038/s41598-021-96530-1. [PubMed: 34453072]
67. Kolobarić N, Drenjančević I, Matić A, Šušnjara P, Mihaljević Z, Mihalj M. Dietary Intake of n-3 PUFA-Enriched Hen Eggs Changes Inflammatory Markers' Concentration and Treg/Th17 Cells Distribution in Blood of Young Healthy Adults-A Randomised Study. Nutrients. 2021 May 28;13(6):1851. doi: 10.3390/nu13061851. [PubMed: 34071714]
68. Perez-Hernandez J, Chiurchiù V, Perruche S, You S. Regulation of T-Cell Immune Responses by Pro-Resolving Lipid Mediators. Front Immunol. 2021 Nov 16; 12:768133. doi: 10.3389/fimmu.2021.768133. [PubMed: 34868025]

Key Points:

- sEH inhibition boosts systemic SPM production.
- TPPU regulates the Th17/Treg imbalance and maintains bone structure.
- Patients with periodontitis exhibit higher levels of sEH in gingivae.

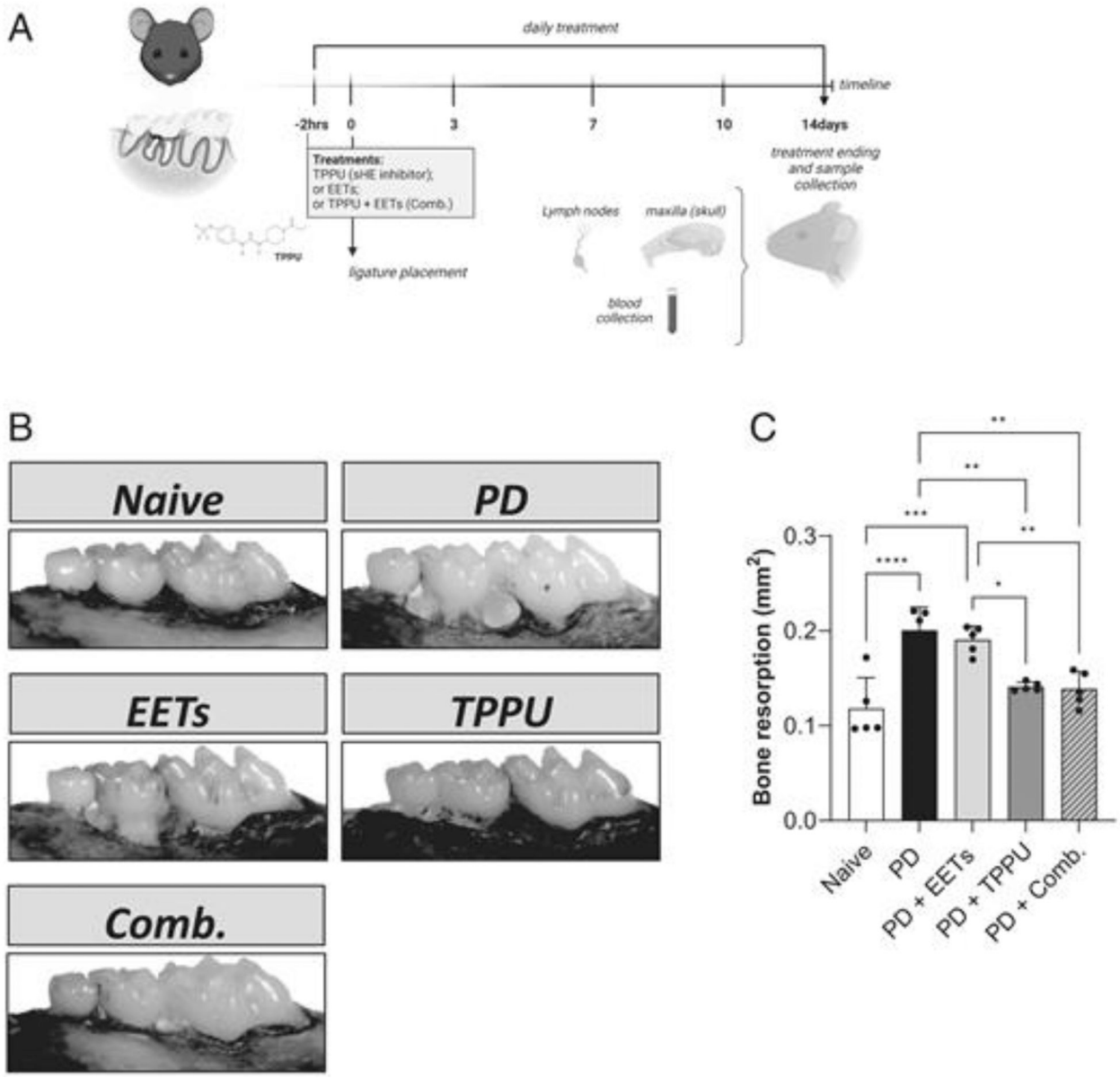

Figure 1.

Evaluation of the impact of sEH inhibition on alveolar bone loss in mice with experimental periodontitis. (A) Experimental design. (B) Representative images of the palatal view of the jaws stained with 10% methylene blue. (C) Quantification of the bone loss (mm2) area refers to the region of the cementoenamel junction and the alveolar bone. Data are expressed as mean ± SD; n = 5 animals per group. Data are pooled from two independent repeat experiments. *p < 0.05, **p < 0.01, ***p < 0.001, ****p < 0.0001.

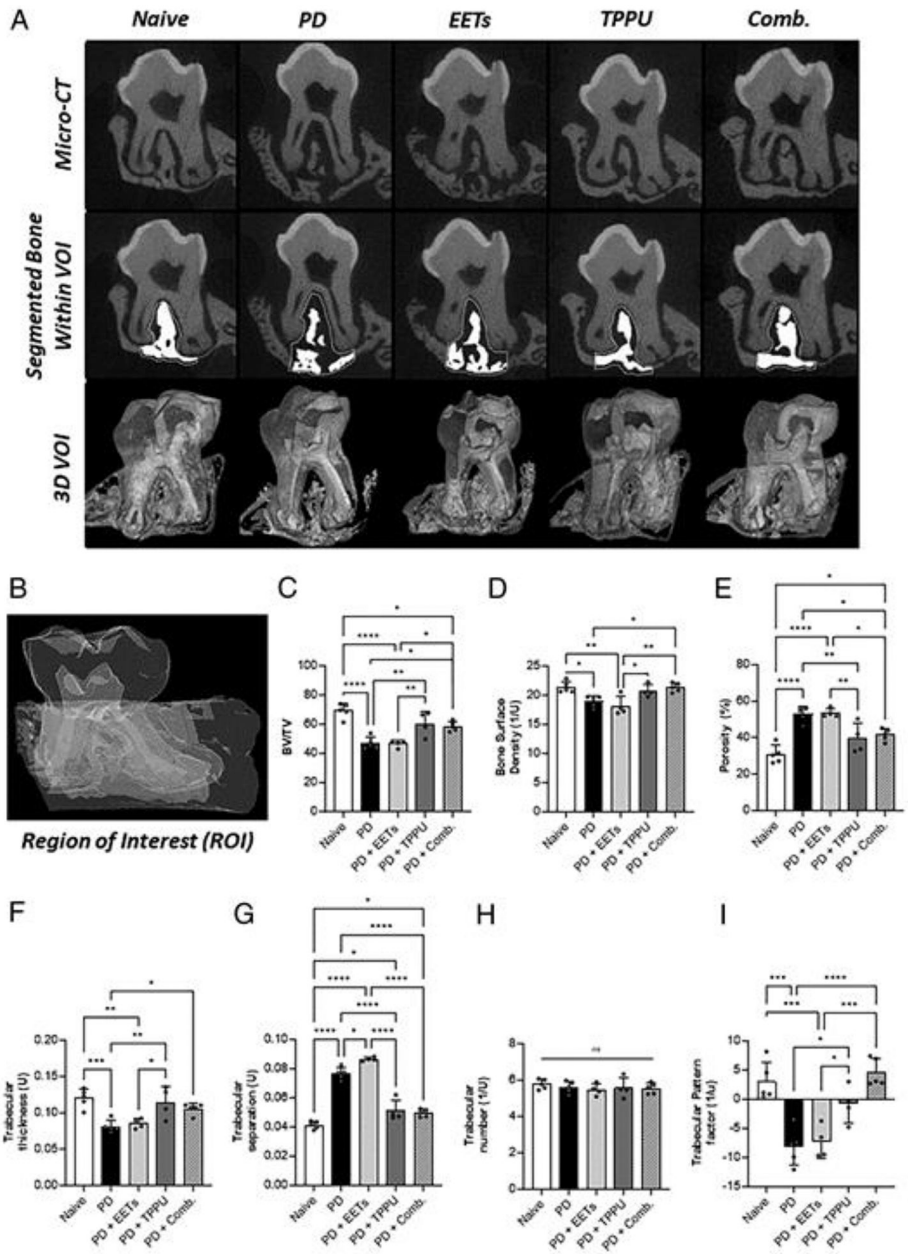

Figure 2.

Pharmacological inhibition of sEH impairs bone parameters. (**A**) Selection and quantification of bone architecture parameters between the evaluated groups. Initially, the images were manually registered. The volume of interest (VOI) between second molar roots was selected considering all samples (dashed in yellow; volume in orange). The bone within the VOI was segmented using a “global threshold” algorithm, and the three-dimensional (3D) morphometric parameters were calculated using the CT-Analyzer software (Bruker, Kontich, Belgium). (**B**) Region of interest. (**C**) Bone density (BV/TV). (**D**) Complexity of bone structure (BS/TV). (**E**) Porosity (Tot.Po). (**F**) Trabecular thickness (Tb.Th). (**G**) Greater medullary spaces (Tb.SP). (**H**) Trabecular bone number. (**I**) Trabecular bone pattern

factor. Data are expressed as mean ± SD; $n = 5$ animals per group. Data are pooled from two independent repeat experiments. *$p < 0.05$, ** $p < 0.01$, ***$p < 0.001$, ****$p < 0.0001$.

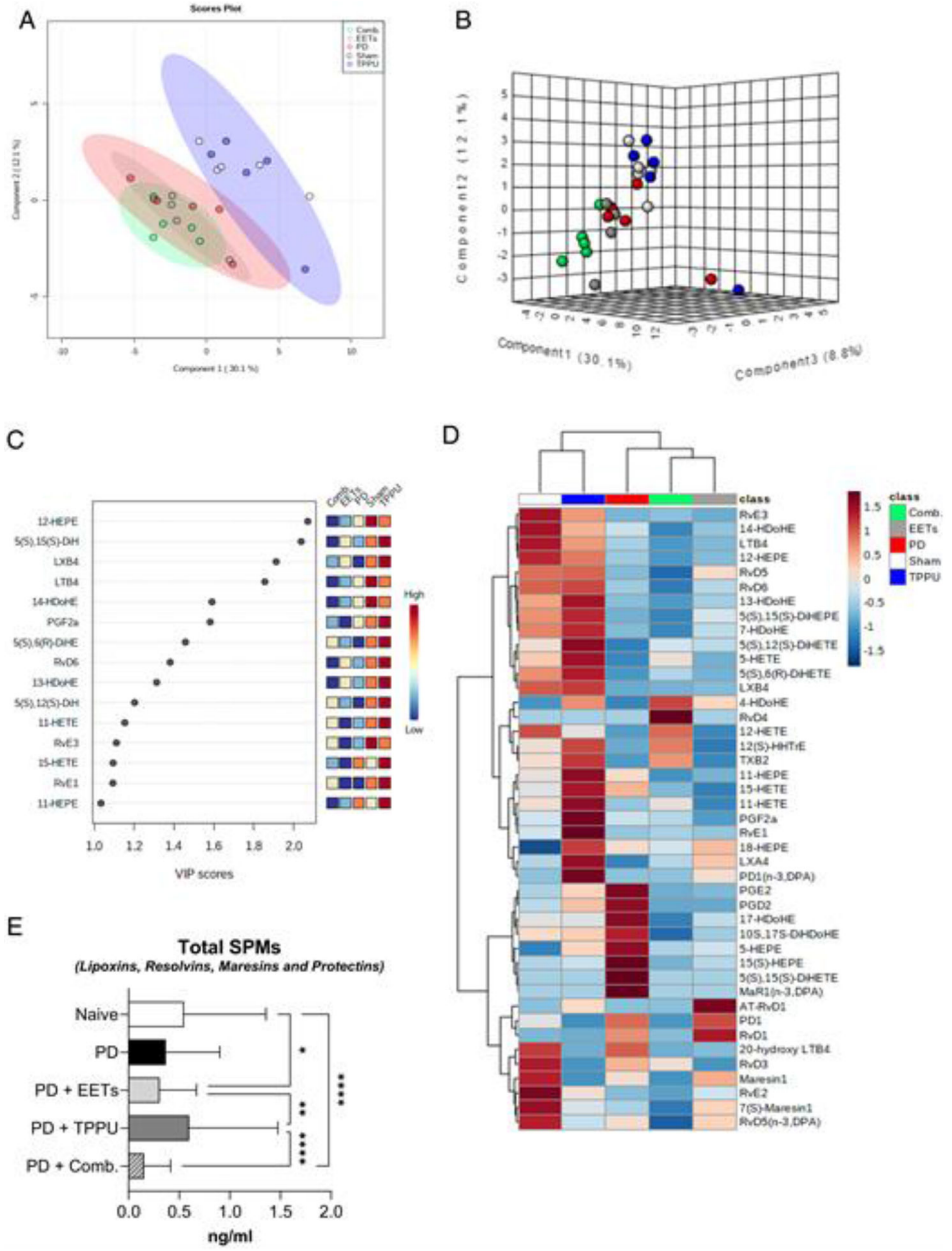

Figure 3.

Inhibition of the sEH enzyme re-established SPM synthesis in blood plasma. (**A** and **B**) Partial least squares discriminant analysis graph in (A) two dimensions and (B) three dimensions for profiles of specialized proresolving lipid mediators (SPMs) and lipid mediators (LMs) in mouse blood plasma. Each point represents a sample in each group. This graph demonstrates groups of samples based on their similarity in LM levels. White circles represent the baseline group, red circles the experimental periodontitis group, gray circles the EETs group, blue circles the sEH inhibitor group (TPPU), and green circles represent the combination group. (**C**) Variable importance in projection (VIP) score and (**D**) heatmap and clustering of SPMs and LMs. (**E**) Total amount of SPMs. Data normalization is shown in

Supplemental Fig. 1. $n = 5$ animals per group. Data are pooled from two independent repeat experiments. *$p < 0.05$, ** $p < 0.01$, ****$p < 0.0001$.

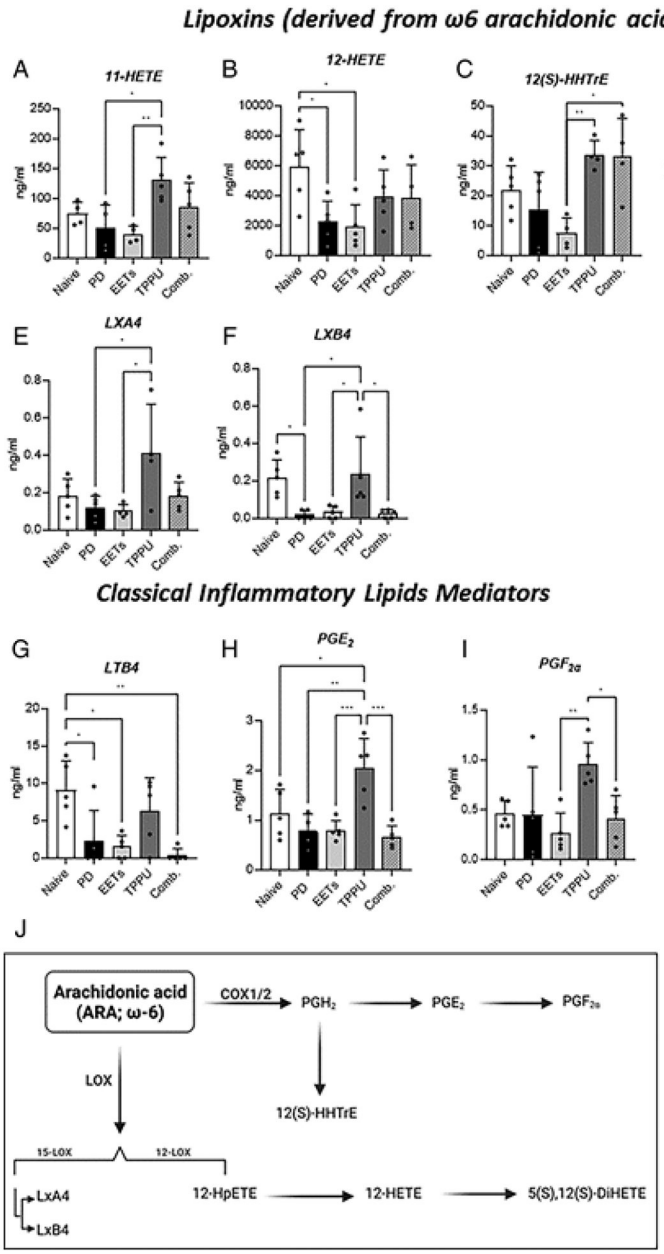

Figure 4.

TPPU influences the synthesis of arachidonic acid cascade mediators and derivatives from ω-6. (**A**–**I**) Univariate one-way ANOVA analysis of (A) 11-HETE, (B) 12-HETE, (C) 12(*S*)-HHTrE, (D) 5(*S*),12(*S*)-DiHETE, (E) LXA_4, (F) LXB_4, (G) leukotriene B_4 (LTB_4), (H) PGE, and (I) $PGF_{2\alpha}$ levels. (**J**) Scheme of metabolic pathways affected by sEH inhibition. Data are expressed as mean ± SD; $n = 5$ animals per group. Data are pooled from two independent repeat experiments. *$p < 0.05$, ** $p < 0.01$, ***$p < 0.001$.

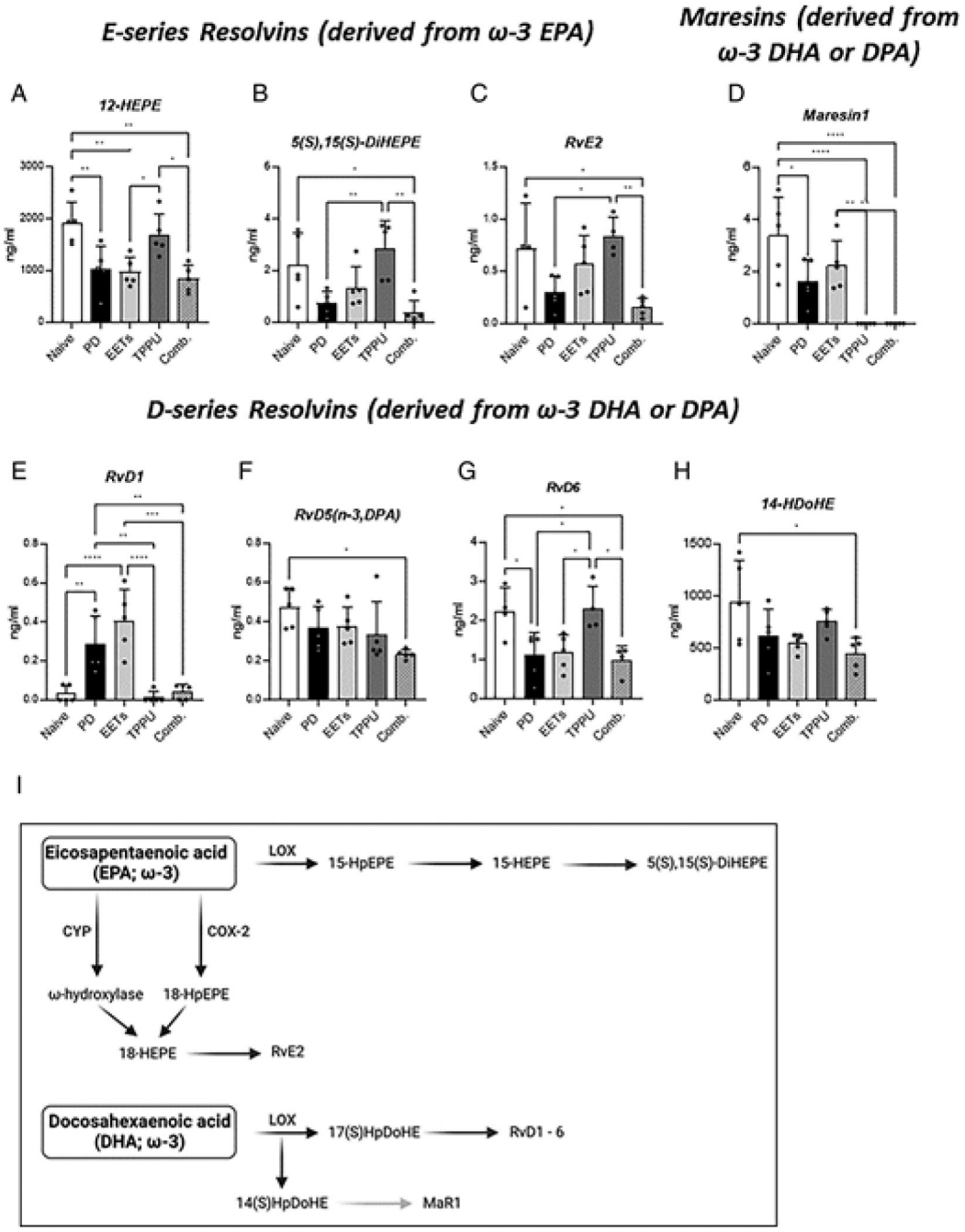

Figure 5.

TPPU influences the synthesis of ω-3–derived eicosapentaenoic acid, docosahexaenoic acid, and docosapentaenoic acid cascade mediators. (**A**–**H**) Univariate one-way ANOVA analysis of levels of (A) 11-HEPE, (B) 5(*S*),15(*S*)-DiHEPE, (C) RvE2 (D) Maresin1, (E) RvD1, (F) RvD5, (G) RvD6, and (H) 14-HDoHE. (**I**) Diagram of metabolic pathways affected by sEH inhibition. Data are expressed as mean ± SD; $n = 5$ animals per group. Data are pooled from two independent repeat experiments. *$p < 0.05$, ** $p < 0.01$, ***$p < 0.001$, ****$p < 0.0001$. DHA, docosahexaenoic acid; DPA, docosapentaenoic acid; EPA, eicosapentaenoic acid.

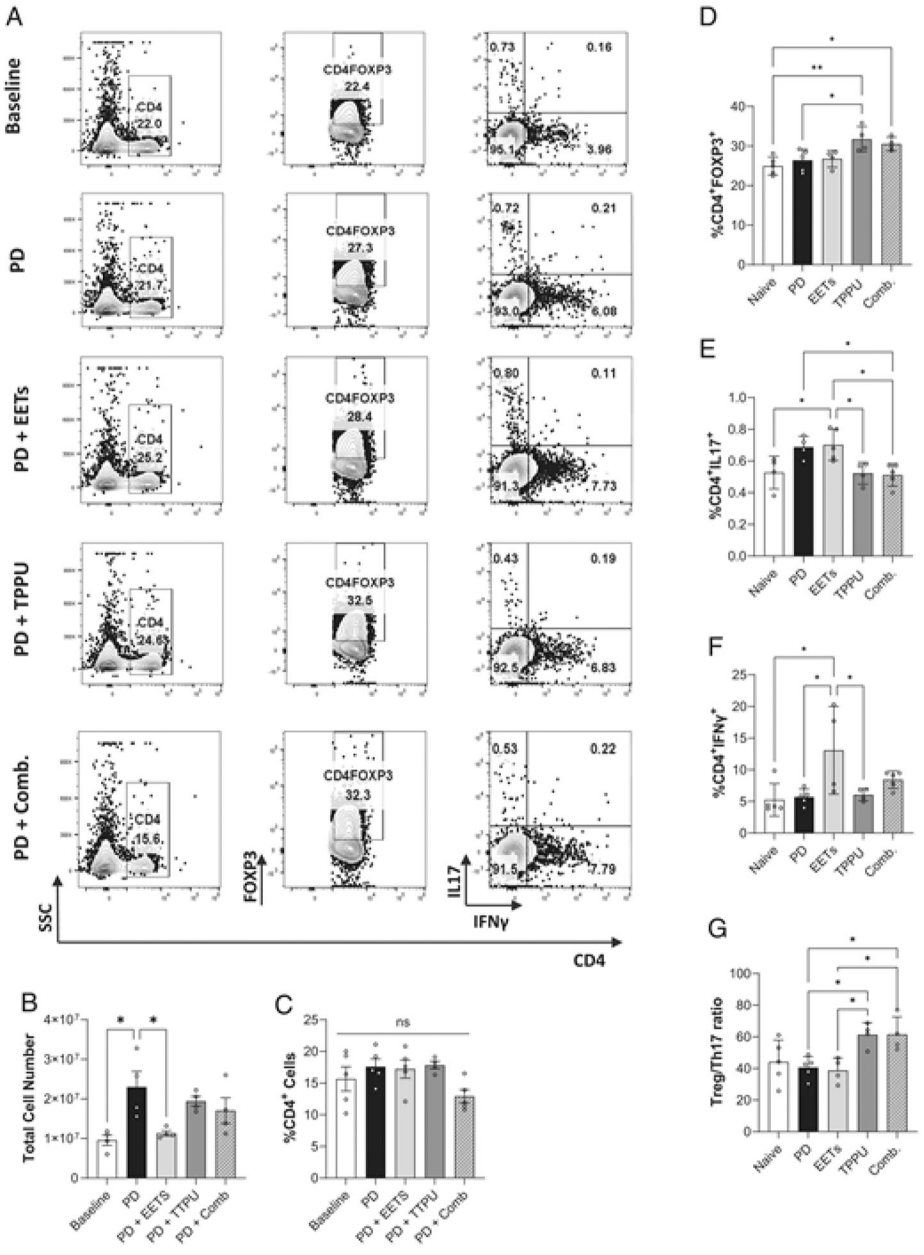

Figure 6.

Regulation of Th17/Treg balance induced by sEH inhibition in cervical lymph nodes. Gate strategy for analyzing the impact of pharmacological inhibition of sEH on the Th17 and Treg profile in cervical lymph nodes. (**A**) Representative plots demonstrating the gating strategy and the percentage of cells. (**B**) Total number of cells in cervical lymph nodes. (**C**–**F**) Percentage of $CD4^+$ (C), $CD4^+Foxp3^+$ (D), $CD4^+IL\text{-}17^+$ (E), and $CD4^+IFN\text{-}\gamma^+$ cells (F). (**G**) Treg/Th17 ratio. Data are expressed as mean ± SD; $n = 5$ animals per group. Data are pooled from two independent repeat experiments. *$p < 0.05$, ** $p < 0.01$.

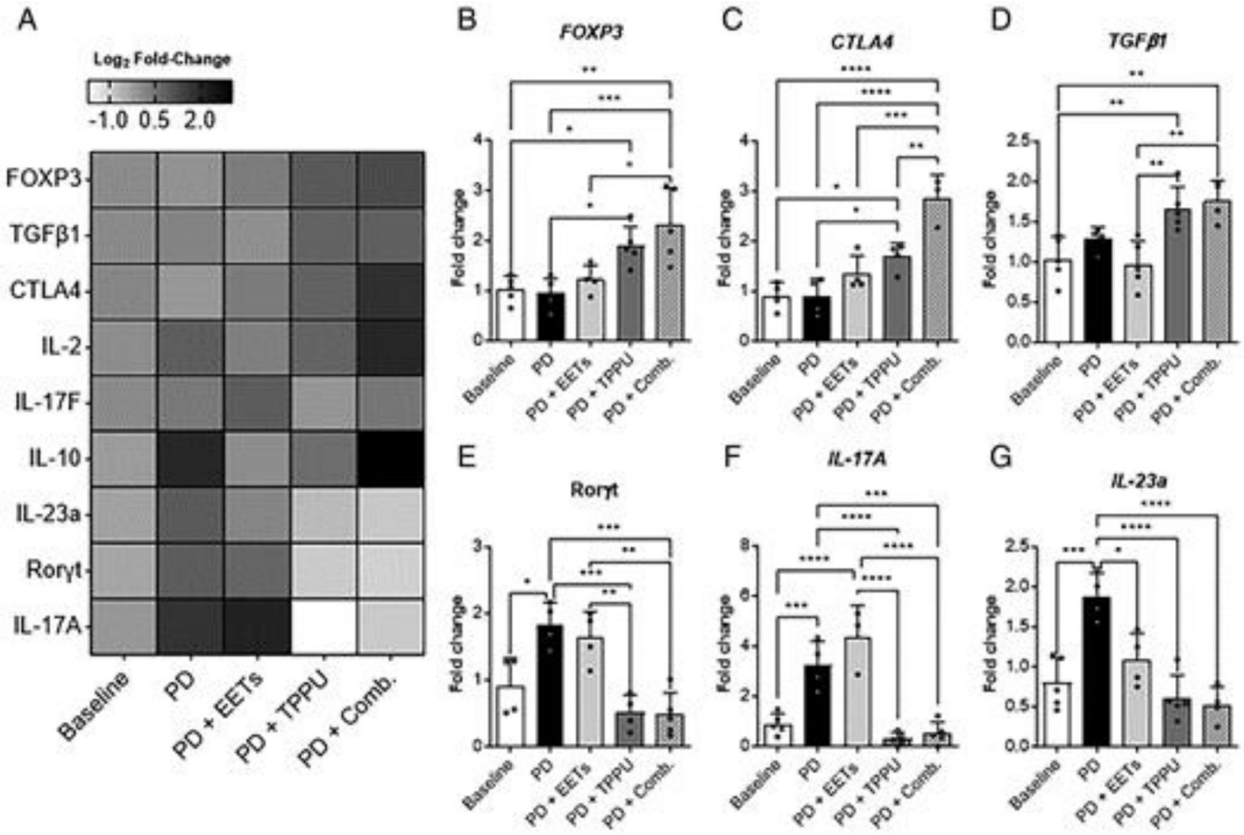

Figure 7.

sEH inhibition induces positive Treg/Th17 balance in cervical lymph nodes. (**A**) Heatmap plotted in $\log_2$ fold change of marker mRNA expression in cervical lymph nodes. (**B**–**G**) mRNA expression of (B) Foxp3, (C) CTLA4, (D) TGF-β1, (E) RORγt, (F) IL-17A, and (G) IL-23a in cervical lymph nodes. Data are expressed as mean ± SD; $n = 5$ animals per group. Data are pooled from two independent repeat experiments. *$p < 0.05$, ** $p < 0.01$, ***$p < 0.001$, ****$p < 0.0001$.

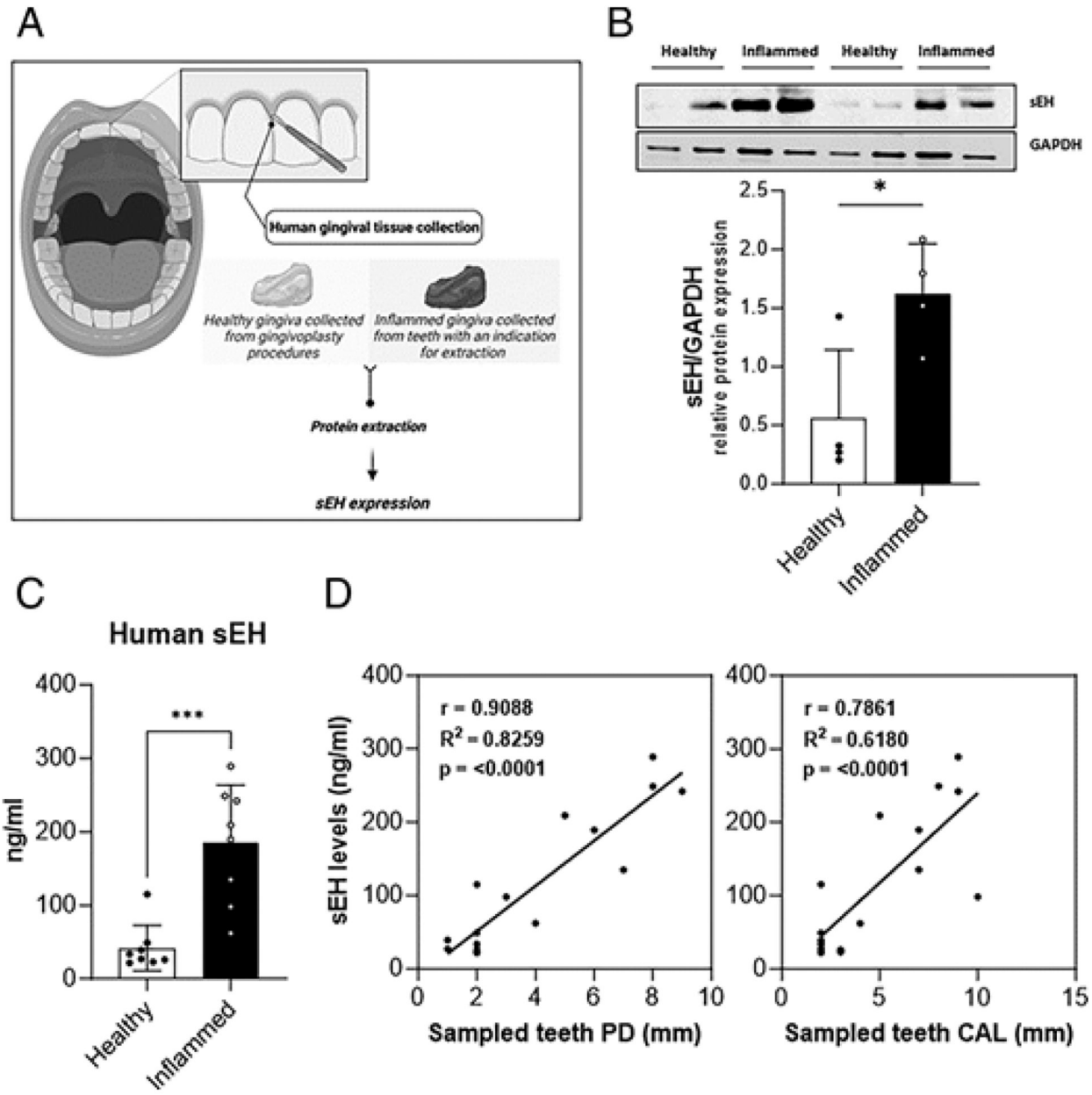

Figure 8.

Increased sEH enzyme expression in inflamed human gingival tissues. (**A**) Experimental design of the collected samples. (A) sEH levels and (**B**) protein expression in healthy and inflamed gingival tissues (periodontitis patients). (**C** and **D**) Correlation with the sEH levels and (C) probing depth and (D) clinical attachment loss. Uncropped Western blotting images are shown in Supplemental Fig. 2. Data are expressed as mean ± SD; $n = 8$ samples per group for ELISA, and $n = 4$ samples per group for Western blotting. $*p < 0.05$, $***p < 0.001$.

Table 1.
Demographic features and periodontal parameters (mean ± SD)

Different letters indicate differences among the groups. BoP, bleeding on probing; CAL, clinical attachment level; FM, full mouth; PD, probing depth.

Variable	Healthy	Inflamed	*p* Value
Sex (male/female)	2/6	5/3	–
Age (y)	40.25 ± 16.19 a	52 ± 15.81 a	0.1641
FM (% of site with plaque)	16.71 ± 13.31 a	69.24 ± 19.86 b	<0.0001
FM (% of site with BoP)	4.5 ± 4.7 a	56.53 ± 17.26 b	0.0010
FM PD (mm)	1.77 ± 0.16 a	3.28 ± 1.02 b	<0.0001
FM CAL (mm)	1.9 ± 0.18 a	4.14 ± 0.92 b	<0.0001
Sampled teeth PD (mm)	1,75 ± 0.46 a	6.25 ± 2.12 b	<0.0001
Sampled teeth CAL (mm)	2.25 ± 0.46 a	7.37 ± 2.06 b	<0.0001